Journal of Applied Analysis and Computation
Volume 12, Number 1, February 2022, 87–105
Website:http://www.jaac-online.com
DOI:10.11948/20210045

STUDIES ON INDIVIDUAL FLUXES VIA POISSON-NERNST-PLANCK MODELS WITH SMALL PERMANENT CHARGES AND PARTIAL ELECTRONEUTRALITY CONDITIONS

Yiwei Wang[1], Lijun Zhang[1] and Mingji Zhang[1,2,†]

Abstract We study a one-dimensional Poisson-Nernst-Planck system for ionic flows through membrane channels with two ion species, one positively charged and one negatively charged. Nonzero but small permanent charges are included. The cross-section area of the channel is included in the system, which provides certain information of the geometry of the three-dimensional channel. This is crucial for our analysis. Of particular interest is to analyze the qualitative properties of the individual fluxes with partial neutral boundary conditions, which provides complementary insights and better understanding of the ionic flow properties. Our study shows that the individual fluxes depend sensitively on multiple system parameters such as permanent charges, channel geometry, boundary conditions (concentrations and potentials) and boundary layers caused by the violation of electroneutrality conditions. Numerical simulations are further performed to provide a more intuitive illustration of our analytical results, and it turns out that numerical results are consistent with our analytical ones.

Keywords PNP, permanent charges, channel geometry, individual fluxes, boundary layers.

MSC(2010) 34A26, 34B16, 34D15, 37D10, 92C35.

1. Introduction

The study of electrodiffusion is an extraordinarily plentiful area for multidisciplinary research with various applications in different research fields, such as physics, chemistry and biology. Mathematical analysis plays essential and unique roles for revealing mechanisms of observed biological phenomena and for discovering new ones, assuming a more or less explicit solution of the associated mathematical model can be achieved. The recent accomplishments ([6, 7, 9, 13, 15, 16, 28, 30, 35, 36, 38, 41, 44, 51, 52, 55]) in analyzing Poisson-Nernst-Planck (PNP) model for ionic flows through membrane channels provides deep insights and better understanding of qualitative properties of ionic flows, especially, the internal dynamics.

†The corresponding author. Email: mingji.zhang@nmt.edu(M. Zhang)
[1]College of Mathematics and Systems Science, Shandong University of Science and Technology, 266510 Qingdao, China
[2]Department of Mathematics, New Mexico Institution of Mining and Technology, Socorro, NM 87801, USA

In this work, we examine boundary layers effects (due to the violation of electroneutrality boundary concentration conditions) on ionic flows via one-dimensional classical PNP models with nonzero but small permanent charges. Of particular interest is to characterize the nonlinear interplays among system parameters, such as channel geometry, small permanent charge, boundary conditions (concentration and potential) and boundary layers.

We comment that the study of the nonlinear interplays among the physical parameters involved in the system provides some efficient ways to control the ionic flows through membrane channels by adjusting boundary conditions, mainly boundary membrane potentials. This is what has been done and doing experimentally in measuring the so-called current-voltage relations, one of the main tools to study ionic flow properties. Correspondingly, it is critical to identify some critical membrane potentials (if possible) that split the potential range into subranges, over which distinct qualitative properties of ionic flows can be observed. The characterization of those critical potentials further depending on other system parameters will provide better understanding of the mechanism of ionic flows though membrane channels, not only mathematically but also experimentally since some critical potentials actually can be estimated experimentally (see Remark 3.2 for more details). On the other hand, the identification of those critical potentials and the resulting subranges will provide excellent choices of initial guessing for numerical studies of the problem, and will be much easier for one to observe distinct and rich properties of ionic flows, which in turn will further help the analysis of the topic.

1.1. Ionic flows and the PNP model

Ion channels are large proteins embedded in cell membrane with a hole down their middle that provides a controllable path for electro-diffusion of ions (mainly Na^+, K^+, Ca^{++} and Cl^-) through biological membranes, establishing communications among cells and the external environment. In this way, ion channels control a wide range of biological functions. Ionic flows are governed by fundamental physical laws of electrodiffusion which relate rates of quantities of interest. Two most relevant biological properties of a channel are permeation and selectivity, both of which are characterized by the current-voltage relations measured experimentally under different ionic conditions. However, for applications, it is important to examine properties of individual fluxes because most experiments (with some exceptions) can only measure the total flux while individual fluxes contain much more information on channel functions [23, 28].

Considering the structural characteristics, the basic continuum model for ionic flows is the PNP system which can be extracted as a reduced model from molecular dynamics ([46]), Boltzmann equations ([3]), and variational principles ([25–27]). The simplest PNP system is the *classical* Poisson-Nernst-Planck (cPNP) system that includes the ideal component $\mu_k^{id}(X)$ in (2.1) only. The ideal component μ_k^{id} contains contributions by considering ion particles as point charges. For a wide range of purposes, the classical PNP models have been simulated and analyzed (see, e.g., [1, 3–5, 11, 12, 21, 24, 43, 45, 47, 48, 50, 53]) extensively. A major weak point of the cPNP is that it treats ions as point-charges, which is reasonable only in very dilute situation. Many important properties of ion channels, such as selectivity, rely on ion sizes critically. To study the ion size effects on ionic flows, one has to take into consideration ion-specific components of the electrochemical potential in PNP

models. PNP-type models with ion sizes have been investigated computationally for ion channels and have shown great success (e.g., [14,17,18,21,22,33,34,49]).

For ionic solutions with n ion species, the PNP system reads

$$\begin{aligned} &\nabla\cdot\Big(\varepsilon_r(\mathbf{r})\varepsilon_0\nabla\Phi\Big)=-e\Big(\sum_{s=1}^{n}z_sc_s+\mathcal{Q}(\mathbf{r})\Big),\\ &\nabla\cdot\mathcal{J}_k=0,\quad -\mathcal{J}_k=\frac{1}{k_BT}\mathcal{D}_k(\mathbf{r})c_k\nabla\mu_k,\quad k=1,2,\cdots,n, \end{aligned} \tag{1.1}$$

where $\mathbf{r}\in\Omega$ with Ω being a three-dimensional cylindrical-like domain representing the channel, $\mathcal{Q}(\mathbf{r})$ is the permanent charge density, $\varepsilon(\mathbf{r})$ is the relative dielectric coefficient, ε_0 is the vacuum permittivity, e is the elementary charge, k_B is the Boltzmann constant, T is the absolute temperature; Φ is the electric potential. Also, for the kth ion species, c_k is the concentration, z_k is the valence (the number of charges per particle), μ_k is the electrochemical potential depending on Φ and $\{c_j\}$, $\mathcal{J}_k$ is the flux density, and $\mathcal{D}_k(\mathbf{r})$ is the diffusion coefficient.

Based on the fact that ion channels have narrow cross-sections relative to their lengths, reduction of the three-dimensional steady-state PNP systems (1.1) to a quasi-one-dimensional models was first proposed in [43] and was rigorosely justified in [40] for special cases. A quasi-one-dimensional steady-state PNP model takes the form

$$\begin{aligned} &\frac{1}{h(x)}\frac{d}{dx}\Big(\varepsilon_r(x)\varepsilon_0h(x)\frac{d\Phi}{dx}\Big)=-e\Big(\sum_{s=1}^{n}z_sc_s+Q(x)\Big),\\ &\frac{d\mathcal{J}_k}{dx}=0,\quad -\mathcal{J}_k=\frac{1}{k_BT}D_k(x)h(x)c_k\frac{d\mu_k}{dx},\quad k=1,2,\ldots,n, \end{aligned} \tag{1.2}$$

where $x\in[0,1]$ is the coordinate along the axis of the channel that is normalized to $[0,1]$, $h(x)$ is the area of cross-section of the channel over the location x.

For system (1.2), we have the following boundary conditions (see [15] for a reasoning), for $k=1,2,\cdots,n$,

$$\Phi(0)=\mathcal{V},\quad c_k(0)=L_k>0;\quad \Phi(1)=0,\quad c_k(1)=R_k>0,\quad k=1,2,\cdots,n. \tag{1.3}$$

1.2. Permanent charges

While some information may be obtained by ignoring the permanent charge and focusing on the effects of boundary conditions, the charges and sizes of ions, etc., we believe that different channel types differ mainly in the distribution of permanent charge ([19]). For both ion channels and semiconductors, permanent charges add an additional component-probably the most important one-to their rich behavior, in particular, for ion channels, a permanent charge reflects the structure of the channel protein. Permanent charge density may depend on the location of many atoms, the shape of the protein (channel geometry), and so on ([16]). In general, the permanent charge $Q(x)$ is modeled by a piecewise constant function, that is, we assume, for a partition $x_0=0<x_1<\cdots<x_{m-1}<x_m=l$ of $[0,l]$ into m subintervals, $Q(x)=Q_j$ for $x\in(x_{j-1},x_j)$ where Q_j's are constants with $Q_1=Q_m=0$ (the intervals $[x_0,x_1]$ and $[x_{m-1},x_m]$ are viewed as the reservoirs without permanent charges).

In [15], under the framework of geometric singular perturbation theory, the existence and uniqueness (local) was established for the boundary value problem (1.2)-(1.3) with one cation and one anion and the permanent charge function modeled by

$$Q(x) = 0 \text{ if } 0 < x < a; \quad Q(x) = Q_0 \text{ if } a < x < b; \quad Q(x) = 0 \text{ if } b < x < 1, \quad (1.4)$$

where Q_0 is some nonzero constant. Due to the challenge in obtaining explicit expressions of the I-V relation with nonzero permanent charges, in [30], the author studied the case with Q_0 in (1.4) being small and employed regular perturbation analysis (viewing Q_0 as a small perturbation to the solutions of the system (1.2)-(1.3)) to further study the effects on ionic flows from the permanent charges. In [9, 55], multiple cations are considered in the PNP model focusing on the competition between cations due to the nonlinear interplays among system parameters, particularly diffusion coefficients, small permanent charges, channel geometry and boundary concentrations. Numerical simulations are performed in [55] to provide more intuitive illustrations for the analytical results. In [51], the authors study the small permanent charge effects on I-V relations via the PNP system with multiple cations. In these works, interesting ionic flow properties are observed and meanwhile the analysis indicates the critical role that the permanent charge plays in the study of ionic flow properties of interest.

1.3. Electroneutrality conditions and boundary layers

To describe the actual behavior of channels or useful transistors, macroscopic reservoirs linked by ion channels must be included ([10, 20–22]). Macroscopic boundary conditions that describe such reservoirs introduce boundary layers of concentration and charge. If those boundary layers reach into the part of the device that performs atomic control, they prominently influence its behavior. Particularly, boundary layers of charge are probably to produce artifacts over long distances because the electric field spreads a long way.

The boundary layer problem should be considered more carefully in the study of such problems, particularly, for ion channel problems. However, very often, when examine the qualitative properties of ionic flows in terms of I-V relations and individual fluxes, which characterize the two most relevant properties (permeation and selectivity) of ion channels, electroneutrality boundary conditions are naturally enforced at both ends of the channel (see, e.g., [1, 6–8, 29–31, 35, 39, 53]), which are defined as

$$\sum_{s=1}^{n} z_s L_s = \sum_{s=1}^{n} z_s R_s = 0. \quad (1.5)$$

Under the condition (1.5), the difficulty in analyzing the dynamics of ionic flows is reduced to a great extent, but the effects on ionic flows from boundary layers that carries much more rich information cannot be examined.

To better understand the mechanism of ionic flows through membrane channels, one need to consider the boundary layer effects during the study. Recently, there are some works focusing on the boundary layer effects on ionic flows via PNP system with zero permanent charge, and much more rich dynamics were observed (see [2, 42, 52, 54]). Due to the sensitivity of electric potentials on boundary layers and

the complexity arising from the nonzero permanent charge, in this work, we consider the PNP problem under the assumption of partial neutral boundary condition, more precisely, we assume

$$-z_2L_2 = \sigma(z_1L_1) \text{ and } -z_2R_2 = z_1R_1, \tag{1.6}$$

where σ is some positive constant not equal to 1 ($\sigma = 1$ in (1.6) implies neutral state). More precisely, we assume the boundary layer just exists at one end of the ion channel, and the other end is still neutral.

We comment that in [15, 36, 37], the authors studied the classical PNP system and established the existence and local uniqueness result for small $\varepsilon > 0$. In the construction of the singular orbit, the solution to the limiting PNP system ($\varepsilon \to 0$), the boundary layer is characterized (see Corollary 3.3 in [15] for example), However, the author did not examine the effects on ionic flows from the boundary layers, which provides complementary information and better understanding of the dynamics of ionic flows through membrane channels.

2. Problem set-up and some previous results

We set up our problem and recall some results from [30], which will be fundamental for our analysis later.

2.1. The steady-state boundary value problem and assumptions

Our main interest is to examine the boundary layer effect on ionic flows via the PNP system (1.2)-(1.3) with small permanent charges.

In this work, we take the same setting as that in [30] but *without* assuming electroneutrality boundary conditions: $z_1L_1 + z_2L_2 = z_1R_1 + z_2R_2 = 0$ on both ends of the ion channel, which includes:

(A1). We consider two charged particles ($n = 2$) with $z_1 > 0$ and $z_2 < 0$.

(A2). The PNP model only includes the ideal component $\mu_i^{id}(X)$ of the electrochemical potential defined by

$$\mu_k^{id}(x) = z_k e\Phi(x) + k_BT \ln \frac{c_k(x)}{c_0}, \tag{2.1}$$

where c_0 is some characteristic number density.

(A3). $\varepsilon_r(X) = \varepsilon_r$ and $\mathcal{D}_i(X) = \mathcal{D}_i$.

We will assume (A1)–(A3) from now on. We first make the following dimensionless rescaling ([30]). Let

$$\phi = \frac{e}{k_BT}\Phi, \quad V = \frac{e}{k_BT}\mathcal{V}, \quad \varepsilon^2 = \frac{\varepsilon_r\varepsilon_0 k_BT}{e^2}, \quad J_k = \frac{\mathcal{J}_k}{D_k}.$$

Correspondingly, the boundary value problem (1.2)-(1.3) becomes

$$\begin{aligned} &\frac{\varepsilon^2}{h(x)}\frac{d}{dx}\left(h(x)\frac{d}{dx}\phi\right) = -z_1c_1 - z_2c_2 - Q(x), \\ &h(x)\frac{dc_k}{dx} + z_k h(x)c_k\frac{d\phi}{dx} = -J_k, \quad \frac{dJ_k}{dx} = 0, \ k = 1, 2 \end{aligned} \tag{2.2}$$

with the boundary conditions

$$\phi(0)=V,\ c_k(0)=L_k;\quad \phi(1)=0,\ c_k(1)=R_k,\ k=1,2. \tag{2.3}$$

We point out that both the variable c and the function $h(x)$ in the equation (2.2) are dimensionless.

2.2. Some previous results

We recall some results from [30] that are critical for our analysis. The authors in [30] treat $|Q_0|$ small compared to the boundary concentrations L_k's and R_k's, and derive approximations for the individual fluxes expanded in Q_0:

$$\mathcal{J}_k(V;Q_0)=\mathcal{J}_{k0}(V)+\mathcal{J}_{k1}(V;\lambda)Q_0+o(Q_0), \tag{2.4}$$

where $\mathcal{J}_k=D_kJ_k$ (correspondingly, $\mathcal{J}_{k0}=D_kJ_{k0}$ and $\mathcal{J}_{k1}=D_kJ_{k1}$) and

$$\begin{aligned}
J_{10}=&\frac{(c_1^L-c_1^R)(z_1V+\ln L_1-\ln R_1)}{H(1)(\ln c_1^L-\ln c_1^R)},\ J_{20}=\frac{(c_2^L-c_2^R)(z_2V+\ln L_2-\ln R_2)}{H(1)(\ln c_2^L-\ln c_2^R)},\\
J_{11}=&\frac{A(z_2(1-B)\lambda+1)}{(z_1-z_2)H(1)}(z_1\lambda+1),\ J_{21}=\frac{A(z_1(1-B)\lambda+1)}{(z_2-z_1)H(1)}(z_2\lambda+1),
\end{aligned} \tag{2.5}$$

with

$$\begin{aligned}
\lambda=&\frac{\phi^L-\phi^R}{\ln c_1^L-\ln c_1^R},\quad A=\frac{(c_1^L-c_1^R)(c_{10}^b-c_{10}^a)}{c_{10}^ac_{10}^b(\ln c_1^L-\ln c_1^R)},\\
B=&\frac{\ln c_{10}^b-\ln c_{10}^a}{A}=\frac{(\ln c_1^L-\ln c_1^R)(\ln c_{10}^b-\ln c_{10}^a)}{(c_1^L-c_1^R)(c_{10}^b-c_{10}^a)}c_{10}^ac_{10}^b.
\end{aligned} \tag{2.6}$$

Here,

$$\begin{aligned}
&\phi^L=V-\frac{1}{z_1-z_2}\ln\frac{-z_2L_2}{z_1L_1},\quad z_1c_1^L=-z_2c_2^L=(z_1L_1)^{\frac{-z_2}{z_1-z_2}}(-z_2L_2)^{\frac{z_1}{z_1-z_2}},\\
&\phi^R=-\frac{1}{z_1-z_2}\ln\frac{-z_2R_2}{z_1L_1},\quad z_1c_1^R=-z_2c_2^R=(z_1R_1)^{\frac{-z_2}{z_1-z_2}}(-z_2R_2)^{\frac{z_1}{z_1-z_2}},\\
&c_{10}^a=c_1^L+\alpha(c_1^R-c_1^L),\quad c_{10}^b=c_1^L+\beta(c_1^R-c_1^L),
\end{aligned} \tag{2.7}$$

where

$$\alpha=\frac{H(a)}{H(1)}\ \text{ and }\ \beta=\frac{H(b)}{H(1)}. \tag{2.8}$$

The quantities J_{11} and J_{21} are the leading terms containing permanent charges and channel geometry effects on individual fluxes and will be studied in detail.

We define the following function, which will be used often in our analysis. For $t>0$, set

$$\begin{aligned}
\gamma(t)=&\frac{\sigma^{\frac{z_1}{z_1-z_2}}t\ln\sigma^{\frac{z_1}{z_1-z_2}}t-\sigma^{\frac{z_1}{z_1-z_2}}t+1}{(\sigma^{\frac{z_1}{z_1-z_2}}t-1)\ln\sigma^{\frac{z_1}{z_1-z_2}}t}\\
&\text{for }\ t\neq\sigma^{-\frac{z_1}{z_1-z_2}}\ \text{ and }\ \gamma(\sigma^{-\frac{z_1}{z_1-z_2}})=\frac{1}{2}.
\end{aligned} \tag{2.9}$$

One establishes easily that

Lemma 2.1. *Assume that $t>0$. One has*

$$0<\gamma(t)<1,\quad \gamma'(t)>0,\quad \lim_{t\to0}\gamma(t)=0\quad \textit{and}\quad \lim_{t\to\infty}\gamma(t)=1.$$

3. Effects from small permanent charges and channel geometry with boundary layers

We now examine the effects on individual fluxes from permanent charges and channel geometry under the assumption (1.6).

3.1. Comparison between zeroth order and first order in Q_0

For the kth ion species, upon introducing μ_k^δ to denote the difference between its electrochemical potentials at the two boundaries, one has

$$\mu_k^\delta := \mu_k^\delta(V; L_k, R_k) = \mu_k(0) - \mu_k(1) = k_B T(z_k V + \ln L_k - \ln R_k). \tag{3.1}$$

Together with the assumption (1.6), equation (2.5) can be rewritten as

$$\begin{aligned}
J_{10} =& \frac{\sigma^{\frac{z_1}{z_1-z_2}} L_1 - R_1}{H(1)\big(\frac{z_1}{z_1-z_2}\ln\sigma + \ln\frac{L_1}{R_1}\big)} \frac{\mu_1^\delta}{k_B T},\\
J_{20} =& -\frac{z_1}{z_2}\frac{\sigma^{\frac{z_1}{z_1-z_2}} L_1 - R_1}{H(1)\big(\frac{z_1}{z_1-z_2}\ln\sigma + \ln\frac{L_1}{R_1}\big)} \frac{\mu_2^\delta}{k_B T},\\
J_{11} =& \frac{A_1\big(z_2(1-B_1)V + (1+\frac{z_2}{z_1-z_2}B_1)\ln\sigma + \ln\frac{L_1}{R_1}\big)}{(z_1-z_2)\big(\frac{z_1}{z_1-z_2}\ln\sigma + \ln\frac{L_1}{R_1}\big)^2 H(1)} \frac{\mu_1^\delta}{k_B T},\\
J_{21} =& \frac{A_1\big(z_1(1-B_1)V + \frac{z_1}{z_1-z_2}B_1\ln\sigma + \ln\frac{L_1}{R_1}\big)}{(z_2-z_1)\big(\frac{z_1}{z_1-z_2}\ln\sigma + \ln\frac{L_1}{R_1}\big)^2 H(1)} \frac{\mu_2^\delta}{k_B T},
\end{aligned} \tag{3.2}$$

where

$$\begin{aligned}
A_1 =& -\frac{(\beta-\alpha)\Big(\sigma^{\frac{z_1}{z_1-z_2}} L_1 - R_1\Big)^2}{\Big((1-\alpha)\sigma^{\frac{z_1}{z_1-z_2}} L_1 + \alpha R_1\Big)\Big((1-\beta)\sigma^{\frac{z_1}{z_1-z_2}} L_1 + \beta R_1\Big)\Big(\frac{z_1}{z_1-z_2}\ln\sigma + \ln\frac{L_1}{R_1}\Big)},\\
B_1 =& \frac{\ln\big((1-\beta)\sigma^{\frac{z_1}{z_1-z_2}} L_1 + \beta R_1\big) - \ln\big((1-\alpha)\sigma^{\frac{z_1}{z_1-z_2}} L_1 + \alpha R_1\big)}{A_1}.
\end{aligned}$$

Remark 3.1. For J_{k1} in (3.2), if $\sigma = 1$, we will get the same results as those under electroneutrality conditions in [30].

For convenience in our following discussion, for $0 < x < 1$ and $t = \frac{L_1}{R_1}$, we introduce

$$\omega(x) = (1-x)\sigma^{\frac{z_1}{z_1-z_2}} t + x, \quad \omega_1(x) = (1-x)t + x. \tag{3.3}$$

3.2. Dependence of signs of J_{k1} on channel geometry

In this section, we study the sign of J_{k1}'s, which further depends on the boundary condition (V, L_k, R_k), the channel geometry (α, β) and the boundary layer in terms of σ.

The sign of A_1 and $1-B_1$ is critical in our following discussion, which is sensitive to other system parameters, particularly, the channel geometry (α, β) and the ration

of boundary concentrations $t = L_1/R_1$. We first consider the sign of $1-B_1$. Assume $t = \frac{L_1}{R_1}$, we rewrite $1 - B_1$ as

$$1 - B_1 = \frac{p(\beta)}{(\beta-\alpha)\big(\sigma^{\frac{z_1}{z_1-z_2}}t - 1\big)^2},$$

where

$$p(\beta) = \omega(\alpha)\omega(\beta)\ln\sigma^{\frac{z_1}{z_1-z_2}}t\ln\frac{\omega(\beta)}{\omega(\alpha)} + (\beta-\alpha)\big(\sigma^{\frac{z_1}{z_1-z_2}}t - 1\big)^2.$$

For $p(\beta)$, the following result can be established.

Lemma 3.1. *Assume $t = \frac{L_1}{R_1} > 1$, $\sigma > 1$ and $\gamma(t)$ be as in (2.9). Then,*

(i) *for $\gamma(t) > \alpha$, there exists a unique $\beta_1 \in (\alpha, 1)$ such that $p(\beta) < 0$ if $\beta \in (\alpha, \beta_1)$ and $p(\beta) > 0$ if $\beta \in (\beta_1, 1)$.*

(ii) *for $\alpha \geq \gamma(t)$, $p(\beta) > 0$.*

It follows that

Lemma 3.2. *Assume $t = \frac{L_1}{R_1} > 1$ and $\sigma > 1$. One has*

(i) *$1 - B_1 > 0$ if either $\gamma(t) > \alpha$ and $\beta \in (\beta_1, 1)$; or $\gamma(t) \leq \alpha$;*

(ii) *$1 - B_1 < 0$ if $\gamma(t) > \alpha$ and $\beta_1 \in (\alpha, \beta_1)$.*

As for the sign of A_1, we have

Lemma 3.3. *Assume $t = \frac{L_1}{R_1} > 1$, $\sigma > 1$ and $\gamma(t)$ be as in (2.9). One has $A_1 < 0$.*

One of our main results then is stated as follows:

Theorem 3.1. *Assume $B_1 \neq 1$. Define V_{1p}^* and V_{2p}^* by $J_{11}(V_{1p}^*) = 0$ and $J_{21}(V_{2p}^*) = 0$, respectively, which are given by*

$$\begin{aligned} V_{1p}^* &= \frac{1}{z_1 - z_2}\Big(\frac{z_1\ln\sigma + (z_1 - z_2)\ln t}{z_2(B_1 - 1)} + \ln\sigma\Big), \\ V_{2p}^* &= \frac{1}{z_1 - z_2}\Big(\frac{z_1\ln\sigma + (z_1 - z_2)\ln t}{z_1(B_1 - 1)} + \ln\sigma\Big). \end{aligned} \tag{3.4}$$

Particularly, $V_{1p}^* - V_{2p}^* = \frac{z_1\ln\sigma + (z_1-z_2)\ln t}{z_1 z_2(B_1-1)}$. Furthermore, for $t = \frac{L_1}{R_1} > 1$, $\sigma > 1$ and $\gamma(t)$ be as in (2.9), one has

(i) *if $\alpha < \gamma(t)$ and $\beta \in (\alpha, \beta_1)$, then, $V_{1p}^* < V_{2p}^*$; and*

(i1) *for $V < V_{1p}^*$, $J_{10}J_{11} > 0$ and $J_{20}J_{21} > 0$;*

(i2) *for $V_{1p}^* < V < V_{2p}^*$, $J_{10}J_{11} < 0$ and $J_{20}J_{21} > 0$;*

(i3) *for $V > V_{2p}^*$, $J_{10}J_{11} < 0$ and $J_{20}J_{21} < 0$.*

Equivalently, for $V < V_{1p}^*$, the (small) positive Q_0 strengthens both $|J_1|$ and $|J_2|$; for $V_{1p}^* < V < V_{2p}^*$, the (small) positive Q_0 reduces $|J_1|$ while strengthens $|J_2|$; and for $V > V_{2p}^*$, the (small) positive Q_0 reduces both $|J_1|$ and $|J_2|$.

(ii) *if either $\alpha < \gamma(t)$ and $\beta \in (\beta_1, 1)$ or $\alpha \geq \gamma(t)$, then $V_{1p}^* > V_{2p}^*$; and*

(ii1) *for $V < V_{2p}^*$, $J_{10}J_{11} < 0$ and $J_{20}J_{21} < 0$;*

(ii2) *for $V_{2p}^* < V < V_{1p}^*$, $J_{10}J_{11} < 0$ and $J_{20}J_{21} > 0$;*

(ii3) *for* $V > V_{1p}^*$, $J_{10}J_{11} > 0$ *and* $J_{20}J_{21} > 0$.

Equivalently, for $V < V_{2p}^*$, *the (small) positive* Q_0 *reduces both* $|J_1|$ *and* $|J_2|$; *for* $V_{2p}^* < V < V_{1p}^*$, *the (small) positive* Q_0 *strengthens* $|J_1|$ *while reduces* $|J_2|$; *and for* $V > V_{1p}^*$, *the (small) positive* Q_0 *strengthens both* $|J_1|$ *and* $|J_2|$.

Remark 3.2. The critical potentials V_{1p}^* and V_{2p}^* that balance the small permanent charge effects is critical in our study, which can be estimated experimentally. Taking the critical potential V_{1p}^* (zero of $J_{11}(V;\sigma)$) for example, one can take an experimental $J_1(V;Q_0;\sigma)$ (although it is challenging to measure compared to the I-V relations) and numerically (or analytically) compute $J_{10}(V;0;\sigma)$ for ideal case, and this allows one to get an estimate of V_{1p}^* by considering the zero of $J_1(V;Q_0;\sigma)-J_{10}(V;0;\sigma)$. Furthermore, they split the electric potential region into three subregions, over which distinct qualitative properties of the individual fluxes J_1 and J_2 are observed. This actually provides an efficient way to control ionic flows (preference of ion channel over different ion species) through ion channels by adjusting boundary conditions. More importantly, from Theorem 3.1, one observes that, depending on the boundary conditions and channel geometry through (α,β), (small) positive permanent charges

- can reduce the cation flux and enhance the anion flux;
- can enhance both cation and anion fluxes;
- can reduce both cation and anion fluxes;
- but cannot enhance the cation flux while reduce the anion flux.

This is consistent with the result obtained in [30] (Theorems 4.7 and 4.8) without boundary layers.

We also would like to point out that, for $k=1,2$, $J_{k1}(V)$ has a common zero with the zeroth order term $J_{k0}(V)$, namely, the potential V_{cp}^{k*} such that $\mu_k^\delta(V_{cp}^{k*})=0$.

To further examine the qualitative properties of ionic flows, we consider the monotonicity of the leading term J_{k1} in the electric potential V. Direct calculation from (3.1) and (3.2) gives

$$\begin{aligned}
\frac{dJ_{11}}{dV} &= \frac{1}{(z_1-z_2)(\frac{z_1}{z_1-z_2}\ln\sigma+\ln\frac{L_1}{R_1})^2H(1)}\bigg(2z_1z_2A_1(1-B_1)V\\
&\quad + z_2A_1(1-B_1)\ln\frac{L_1}{R_1}+z_1A_1\Big(\Big(1+\frac{z_2}{z_1-z_2}B_1\Big)\ln\sigma+\ln\frac{L_1}{R_1}\Big)\bigg),\\
\frac{d^2J_{11}}{dV^2} &= \frac{2z_1z_2A_1(1-B_1)}{(z_1-z_2)\big(\frac{z_1}{z_1-z_2}\ln\sigma+\ln\frac{L_1}{R_1}\big)^2H(1)},\\
\frac{dJ_{21}}{dV} &= \frac{1}{(z_2-z_1)\big(\frac{z_1}{z_1-z_2}\ln\sigma+\ln\frac{L_1}{R_1}\big)^2H(1)}\bigg(2z_1z_2A_1(1-B_1)V\\
&\quad + z_1A_1(1-B_1)\Big(\ln\sigma+\ln\frac{L_1}{R_1}\Big)+z_2A_1\Big(\frac{z_1}{z_1-z_2}B_1\ln\sigma+\ln\frac{L_1}{R_1}\Big)\bigg),\\
\frac{d^2J_{21}}{dV^2} &= \frac{2z_1z_2A_1(1-B_1)}{(z_2-z_1)\big(\frac{z_1}{z_1-z_2}\ln\sigma+\ln\frac{L_1}{R_1}\big)^2H(1)},
\end{aligned}$$

from which, together with Lemmas 3.2 and 3.3, one has

Proposition 3.1. *Assume $t = \frac{L_1}{R_1} > 1$ and $\sigma > 1$. Let $\gamma(t)$ be as in (2.9). Then,*

(i) *There exists a unique critical point V_{1p}^c such that $\frac{dJ_{11}}{dV}|_{V=V_{1p}^c} = 0$. Furthermore,*

(i1) *$J_{11}(V)$ decreases over $(-\infty, V_{1p}^c)$ and increases over (V_{1p}^c, ∞) if either $\gamma(t) > \alpha$ and $\beta \in (\beta_1, 1)$ or $\gamma(t) \le \alpha$;*

(i2) *$J_{11}(V)$ increases over $(-\infty, V_{1p}^c)$ and decreases over (V_{1p}^c, ∞) if $\gamma(t) > \alpha$ and $\beta \in (\alpha, \beta_1)$;*

(ii) *There exists a unique critical point V_{2p}^c such that $\frac{dJ_{21}}{dV}|_{V=V_{2p}^c} = 0$. Furthermore,*

(ii1) *$J_{21}(V)$ increases over $(-\infty, V_{2p}^c)$ and decreases over (V_{2p}^c, ∞) if either $\gamma(t) > \alpha$ and $\beta \in (\beta_1, 1)$ or $\gamma(t) \le \alpha$;*

(ii2) *$J_{21}(V)$ decreases over $(-\infty, V_{2p}^c)$ and increases over (V_{2p}^c, ∞) if $\gamma(t) > \alpha$ and $\beta \in (\alpha, \beta_1)$;*

Remark 3.3. The identification of the critical potentials V_{kp}^* and V_{kp}^c are crucial, these critical potentials split the electric potential region into several subregions, over which different dynamics of individual fluxes are able to be observed. More importantly, this provides some efficient ways to adjust/control the ionic flows through membrane channels.

3.3. Relations among critical potentials

We next discuss the orders among the critical potentials V_{1p}^* and V_{2p}^* with boundary layers and the ones V_q^1 and V_q^2 under electroneutrality conditions identified in [30].

3.3.1. Critical potentials: neutral conditions vs boundary layers

Recall from (3.4) that

$$V_{1p}^* = \frac{1}{z_1 - z_2}\Big(\frac{z_1 \ln\sigma + (z_1 - z_2)\ln t}{z_2(B_1 - 1)} + \ln\sigma\Big),$$
$$V_{2p}^* = \frac{1}{z_1 - z_2}\Big(\frac{z_1 \ln\sigma + (z_1 - z_2)\ln t}{z_1(B_1 - 1)} + \ln\sigma\Big),$$

and from [30] (formula (4.8) in Theorem 4.8) that

$$V_q^1 = -\frac{\ln L_1 - \ln R_1}{z_2(1 - B)} \quad \text{and} \quad V_q^2 = -\frac{\ln L_1 - \ln R_1}{z_1(1 - B)}.$$

We point out that if $\sigma = 1$, then, $V_{1p}^* = V_q^1$ and $V_{2p}^* = V_q^2$.

Proposition 3.2. *Let $t = \frac{L_1}{R_1} > 1$. For $\sigma > 1$, one has $V_{1p}^* < V_q^1$ and $V_q^2 < V_{2p}^*$.*

Proof. We just prove $V_{1p}^* < V_q^1$, and the other can be discussed similarly. From (3.4), one has

$$V_{1p}^* = \frac{1}{z_1 - z_2}\Big(\frac{z_1 \ln\sigma + (z_1 - z_2)\ln t}{z_2(B_1 - 1)} + \ln\sigma\Big).$$

Considering V_{1p}^* as a function of σ, and let F be the first derivative of V_1^* with respect to σ at $\sigma = 1$, then, we have

$$F = \frac{dV_{1p}^*}{d\sigma}|_{\sigma=1} = \frac{p_1(\beta)}{(z_1 - z_2)z_2 g^2(\beta)},$$

where

$$g(\beta)=\omega_1(\alpha)\omega_1(\beta)\ln t\ln\frac{\omega_1(\beta)}{\omega_1(\alpha)}+(\beta-\alpha)(t-1)^2,$$
$$p_1(\beta)=z_1(\alpha-\beta)\Big[(\beta-\alpha)(t-1)^2\big((t-1)^2+t\ln^2 t\big)+(t^2-t)\big((\beta+\alpha)(1-t)+2t\big)\ln^2 t\ln\frac{\omega_1(\beta)}{\omega_1(\alpha)}\Big]+z_2g^2(\beta).$$

It is easy to check that

$$\lim_{\beta\to\alpha}p_1(\beta)=0,\quad \lim_{\beta\to\alpha}p_1'(\beta)=0,\quad \lim_{\beta\to\alpha}p_1''(\beta)=2(t-1)^2p_2(\alpha),$$

where

$$p_2(\alpha)=(z_2-z_1)(t-1)^2+z_1t\ln^2 t-z_2\omega_1^2(\alpha)\ln^2 t+2z_2(1-t)\omega_1(\alpha)\ln t.$$

Direct calculation shows that $p_2(\alpha)$ is a quadratic function in α, and concave upward, whose discriminant is

$$\triangle=4z_2(t-1)^2[(2z_2-z_1)(t-1)^2+z_1t\ln^2 t]\ln^2 t>0.$$

This indicates $p_2(\alpha)=0$ has two roots, say α_1^* and α_2^* with $\alpha_1^*<\alpha_2^*$ for convenience. Direct calculation shows that $\alpha_1^*>1$. Together with $p_2(1)>0$, one has $p_2(\alpha)>0$ for $0<\alpha<1$, and hence, $\lim_{\beta\to\alpha}p_1''(\beta)>0$. It then follows that $F<0$. Therefore, $V_{1p}^*<V_q^1$ if $\sigma>1$. □

3.3.2. Total order of critical potentials

We provide a total order of the critical potentials V_k^* and V_q^k for $k=1,2$, that split the potential region into subregions, from which one can further study the qualitative properties of ionic flows and examine the effects from boundary layers.

To get started, we introduce a function defined in [30], which will be used in our following discussion. For $t>0$, set

$$\gamma_1(t)=\frac{t\ln t-t+1}{(t-1)\ln t}\ \text{for } t\neq 1,\ \text{and } \gamma_1(1)=\frac{1}{2}. \tag{3.5}$$

One has

Lemma 3.4. *For $t>0$,*

$$0<\gamma_1(t)<1,\ \gamma_1'(t)>0,\ \lim_{t\to 0}\gamma_1(t)=0 \text{ and } \lim_{t\to\infty}\gamma_1(t)=1.$$

Lemma 3.5. *Assume $t=\frac{L_1}{R_1}>1$ and $\gamma_1(t)$ be as in (3.5). Then,*

(i) *for $\alpha<\gamma_1(t)$, there exists a unique $\beta_2\in(\alpha,1)$ such that $1-B<0$ if $\beta\in(\alpha,\beta_2)$ and $1-B>0$ if $\beta\in(\beta_2,1)$.*

(ii) *for $\alpha\geq\gamma_1(t)$, $1-B>0$.*

Theorem 3.2. *Let $t=\frac{L_1}{R_1}>1$ and $\sigma>1$. Suppose $\alpha<\beta_2<\beta_1<1$. One has*

(i) $V_q^2 < V_{2p}^* < V_{1p}^* < V_q^1$ *under one of the following conditions*
  (i1) $\alpha \geq \gamma(t)$*;*
  (i2) $\alpha < \gamma(t)$ *and* $\beta \in (\beta_1, 1)$*;*
(ii) $V_{1p}^* < V_q^1 < V_q^2 < V_{2p}^*$ *if* $0 < \alpha < \gamma_1(t)$ *and* $\beta \in (\alpha, \beta_2)$.

Proof. Notice that $0 < \gamma_1(t) < \gamma(t) < 1$ with $t = \frac{L_1}{R_1} > 1$ and $\sigma > 1$. The result follows directly from Theorem 3.1 and Proposition 3.2. □

To end this section, we would like to further comment that the identification of those critical potentials is significant in the study of ionic flow properties of interest, not only analytically, but also numerically and even experimentally (see also Remark 3.2 for some discussion). As stated in the introduction, two most relevant properties of ion channels are

3.4. Numerical simulations

In this part, numerical simulations are performed to provide more intuitive illustrations of some analytical results. To be specific, we numerically identify the critical potentials V_{kp}^* with boundary layers and V_q^k under electroneutrality conditions, and further verify some analytical results stated in Theorem 3.1, Proposition 3.2 and Theorem 3.2 for some carefully selected system parameters. Other related results can also be numerically illustrated by choosing different parameter values, and we leave that to interested readers.

To get started, we rewrite the system (2.2)-(2.3) as a system of first order ordinary differential equations. Upon introducing $u = \varepsilon\dot{\phi}$ and $\tau = x$, one has

$$\begin{aligned} &\varepsilon\dot{\phi} = u, \quad \varepsilon\dot{u} = -z_1c_1 - z_2c_2 - Q(x) - \varepsilon\frac{h_x(x)}{h(x)}u, \\ &\varepsilon\dot{c}_1 = -z_1c_1u - \varepsilon\frac{J_1}{h(x)}, \quad \varepsilon\dot{c}_2 = -z_2c_2u - \varepsilon\frac{J_2}{h(x)}, \\ &\dot{J}_1 = \dot{J}_2 = 0, \quad \dot{\tau} = 1 \end{aligned} \tag{3.6}$$

with boundary conditions

$$\phi(0) = V,\ c_k(0) = L_k; \quad \phi(1) = 0,\ c_k(1) = R_k,\ k = 1, 2. \tag{3.7}$$

Remark 3.4. We use "bvp4c" in Matlab ([32]), an adaptive mesh solver, for our BVP (3.6)-(3.7), which can efficiently take care of the jumps of $Q(x)$ and $\frac{dh}{dx}$ at the points $x = a$ and $x = b$ by adjusting the mesh points at each stage in the iterative procedure. On the other hand, we take the great advantage from our analysis and the one in [15] that provide very good initial guess for our simulation (see Section 3.2 in [39] for more detailed discussion of the BVP solver and the choice of initial guess).

In our simulations to system (3.6)-(3.7), we take $z_1 = -z_2 = 1,\ L_1 = 20,\ R_1 = 5,\ \varepsilon = 0.01,\ Q_0 = 0.01,\ a = 0.7,\ b = 0.82,$

$$Q(x) = \begin{cases} 0, & 0 < x < a, \\ Q_0, & a < x < b, \\ 0, & b < x < 1, \end{cases} \quad \text{and} \quad h(x) = \begin{cases} \pi\big(-x + r_0 + a\big)^2, & 0 \leq x < a, \\ \pi r_0^2, & a \leq x < b, \\ \pi\big(x + r_0 - b\big)^2, & b \leq x < 1. \end{cases}$$

Remark 3.5. The choice of $h(x)$ is based on the fact that the ion channel is cylindrical-like, and the variable cross-section area is chosen to reflect the fact that the channel is not uniform and much narrower in the neck ($a < x < b$) than other regions ([30]). We further take $r_0 = 0.5$ and the function $h(x)$ is then continuous at the jumping points $x = a$ and $x = b$. Different models for $h(x)$ may be chosen, and similar numerical results should be obtained.

Under the above set-up, direct calculations gives, at $t = L_1/R_1 = 4$,

$$\alpha = \frac{H(a)}{H(1)} = 0.536133,\ \beta = \frac{H(b)}{H(1)} = 0.756713,\ \gamma_1(t) = 0.612175,\ \gamma(t) = 0.611986,$$
$$\beta_1 = 0.678828,\ \beta_2 = 0.678507,$$

from which one has

$$\alpha < \gamma(t) < \gamma_1(t) < \beta_2 < \beta_1 < \beta < 1 \tag{3.8}$$

for $\sigma = 1.005$ in our numerical simulations.

It turns out that our numerical simulations with nonzero but small ε are consistent with our analytical results. To be specific,

(i) We numerically identified the critical potentials V_{1p}^* and V_{2p}^* defined in Theorem 3.1 (first row in Figure 1 with $\sigma = 1.005$; and also identified the critical potentials V_q^1 and V_q^2 identified in [30] (second row in Figure 1) with $\sigma = 1$, that is, under the electroneutrality boundary conditions, from which one can tell the effects from the existence of boundary layers. Furthermore, one can see that $V_q^2 < V_{2p}^* < V_{1p}^* < V_q^1$, which is consistent with Proposition 3.2 (statement (i) satisfying the condition (i2)). The monotonicity of the terms J_{k1} can also be observed from Figure 1, which is consistent with the analytical result stated in Proposition 3.1 (statement (i1) for J_{11} and statement (ii1) for J_{21}).

(ii) Our numerical results show that (see the left figure in Figure 3), with $\sigma = 1.005$,

  (a) $J_1(V;0;\varepsilon)[J_1(V;Q_0;\varepsilon) - J_1(V;0;\varepsilon)] < 0$ (resp. $J_1(V;0;\varepsilon)[J_1(V;Q_0;\varepsilon) - J_1(V;0;\varepsilon)] > 0$) if $V < V_{1p}^*$ (resp. $V > V_{1p}^*$);

  (b) $J_2(V;0;\varepsilon)[J_2(V;Q_0;\varepsilon) - J_2(V;0;\varepsilon)] < 0$ (resp. $J_2(V;0;\varepsilon)[J_2(V;Q_0;\varepsilon) - J_2(V;0;\varepsilon)] > 0$) if $V < V_{2p}^*$ (resp. $V > V_{2p}^*$).

  Furthermore, it is clear that $V_{2p}^* < V_{1p}^*$ and

  (c) $J_k(V;0;\varepsilon)[J_k(V;Q_0;\varepsilon) - J_k(V;0;\varepsilon)] < 0$ for $k = 1, 2$, if $V < V_{2p}^*$;

  (d) $J_1(V;0;\varepsilon)[J_1(V;Q_0;\varepsilon) - J_1(V;0;\varepsilon)] < 0$ while $J_2(V;0;\varepsilon)[J_2(V;Q_0;\varepsilon) - J_2(V;0;\varepsilon)] > 0$ if $V_{2p}^* < V < V_{1p}^*$;

  (e) $J_k(V;0;\varepsilon)[J_k(V;Q_0;\varepsilon) - J_k(V;0;\varepsilon)] > 0$ for $k = 1, 2$ if $V > V_{1p}^*$;

  equivalently, (small) positive Q_0 reduces both $|J_1|$ and $|J_2|$ if $V < V_{2p}^*$; strengthens $|J_2|$ while reduces $|J_1|$ if $V_{2p}^* < V < V_{1p}^*$; and strengthens both $|J_1|$ and $|J_2|$ if $V > V_1^*$. This is consistent with our analytical result stated in (ii) of Theorem 3.1. Here, we use $J_k(V;0;\varepsilon)$ to approximate $J_{k0}(V;0,0)$, and $J_k(V;Q_0;\varepsilon) - J_k(V;0;\varepsilon)$ to approximate $J_{k1}(V;0;0)$, the leading term in our analysis that contains small permanent charge effects.

(iii) Our numerical simulations also show that $J_k(V;0)$ and $J_k(V;Q_0) - J_k(V;0)$ have a common zero (can be seen from Figures 1, 2 and 3), which is consistent with our analytical result (see Remark 3.2). More precisely, this corresponds to the critical values V_{cp}^{1*} from Figure 1 and V_{cp}^{10*} from Figure 2. Due to the perturbation from the higher order terms in Q_0, these two numerically identified critical values are close but not equal, while for our analytical result, they are equal (up to the first order in Q_0, no higher order contributions from Q_0). Similar argument applies to the case under electroneutrality boundary conditions (see equations (4.4) and (4.5) in [30]).

To end this section, we would like to point out that the challenge in our simulation is the selection of the values for a and b, which directly affect the interplay between the small permanent charges and the channel geometry in terms of $(\alpha, \beta) = (H(a)/H(1), H(b)/H(1))$. The numerical simulation not only supports our analytical results, but also provides more intuitive illustrations for our results. Interested readers can choose different values for the parameters a and b to observe other properties stated in this work.

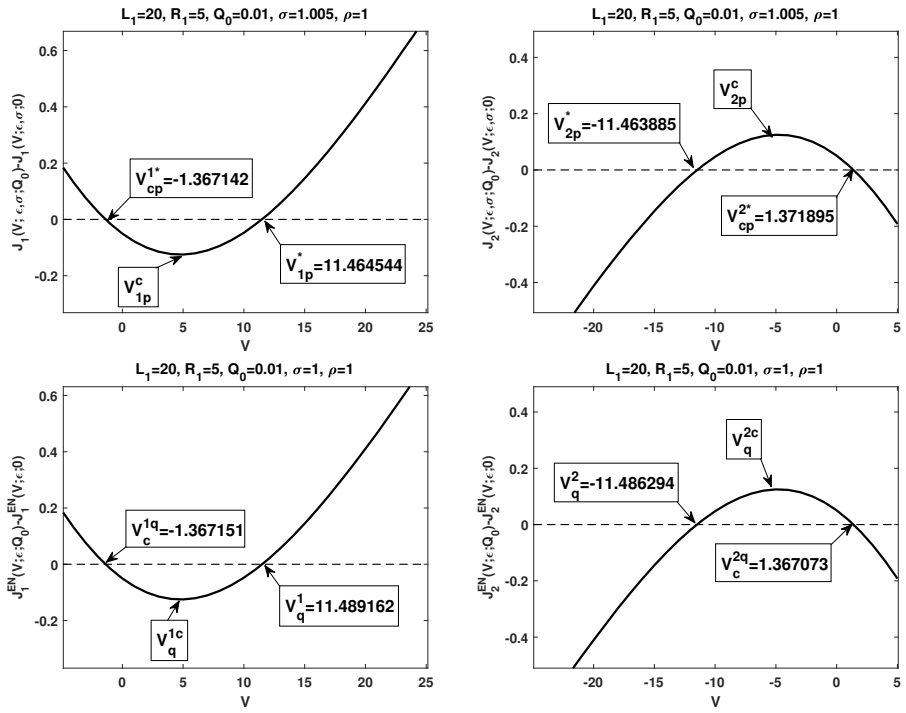

Figure 1. Identification of critical potentials V_{kp}^* with boundary layers and V_q^k under electroneutrality boundary conditions for small $\varepsilon = 0.01$. We also point out that V_{cp}^{k*} is a common zero with $J_k(V;0)$ with boundary layers while V_c^{kq} is a common zero with $J_k(V;0)$ under electroneutrality boundary conditions, see Figure 2. One can easily see that for $(\sigma, \rho) = (1.005, 1.0)$, $V_q^1 - V_{1p}^* = 0.024618$ and $V_q^2 - V_{2p}^* = -0.022409$. This shows clearly the important role played by the boundary layers in the study of ionic flows through membrane channels.

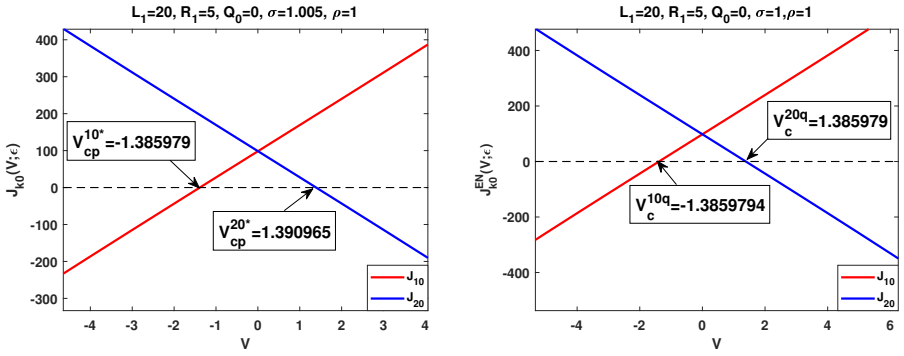

Figure 2. Numerical simulations to $J_{k0}(V)$ for both the case with boundary layers and the one under electroneutrality boundary conditions by $J_k(V;0)$ with $\varepsilon = 0.01$. Critical potentials V_{cp}^{k0*} and V_c^{k0q} are identified. From Figure 1, one can see that V_{cp}^{k0*} is close to V_{cp}^{k*}, and V_c^{k0q} is close to V_c^{kq} (see the discussion in (iii) for more details).

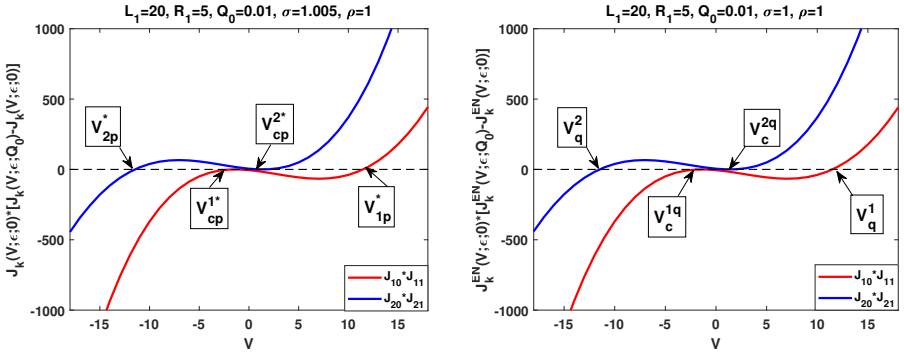

Figure 3. Orders of the critical potentials V_{kp}^* with boundary layers and V_q^k under electroneutrality boundary conditions, respectively for $k = 1, 2$ with $\varepsilon = 0.01$. Under our set-up, the result with boundary layers is consistent with statement (ii) in Theorem 3.1, and the one under electroneutrality boundary conditions is also consistent with statement (ii) in Theorem 4.8 of [30] with β_1 replaced by β_2 under current set-up.

4. Concluding Remarks

We study the Poisson-Nernst-Planck model that includes nonzero but small permanent charges for two ion species, one positively charged and one negatively charged. Of particular interest is to examine the boundary layer effects on individual fluxes due to the violation of electroneutrality boundary conditions at one end of the ion channel. A unique feature of this work is its capability of providing detailed information of the nonlinear interactions among physical parameters involved in the model, such as boundary conditions (concentrations and potentials), small permanent charges and channel geometry, for the individual fluxes. Several critical potentials are identified, and those critical values split the potential region into different subregions, over which distinct qualitative properties of individual fluxes are observed. Moreover, the characterization of these critical potentials is also crucial for future numerical studies on the problem since it provides the best choices of initial guessing. The study in this work could provide important insights to further understand the mechanism of ionic flows through membrane channels, in particu-

lar, the internal dynamics of ionic flows, which cannot be discerned with current technology.

Acknowledgments

Y. Wang thanks the Math Department at NMT for the hospitality during her one-year visit to the department when this work was started. Y. Wang also thanks Dr. Mingji Zhang for bringing her to such an interesting research field.

References

[1] N. Abaid, R. S. Eisenberg and W. Liu, *Asymptotic expansions of I-V relations via a Poisson-Nernst-Planck system*, SIAM J. Appl. Dyn. Syst., 2008, 7, 1507–1526.

[2] R. Aitbayev, P. W. Bates, H. Lu, L. Zhang and M. Zhang, *Mathematical studies of Poisson-Nernst-Planck systems: dynamics of ionic flows without electroneutrality conditions*, J. Comput. Appl. Math., 2019, 362, 510–527.

[3] V. Barcilon, *Ion flow through narrow membrane channels: Part I*, SIAM J. Appl. Math., 1992, 52, 1391–14041.

[4] V. Barcilon, D. Chen and R. S. Eisenberg, *Ion flow through narrow membrane channels: Part II*, SIAM J. Appl. Math., 1992, 52, 1405–1425.

[5] V. Barcilon, D. Chen, R. S. Eisenberg and J. W. Jerome, *Qualitative properties of steady-state Poisson-Nernst-Planck systems: Perturbation and simulation study*, SIAM J. Appl. Math., 1997, 57, 631–648.

[6] P. W. Bates, J. Chen and M. Zhang, *Dynamics of ionic flows via Poisson-Nernst-Planck systems with local hard-sphere potentials: Competition between cations*, Math. Biosci. Eng., 2020, 17, 3736–3766.

[7] P. W. Bates, Y. Jia, G. Lin, H. Lu and M. Zhang, *Individual flux study via steady-state Poisson-Nernst-Planck systems: Effects from boundary conditions*, SIAM J. Appl. Dyn. Syst., 2017, 16, 410–430.

[8] P. W. Bates, W. Liu, H. Lu and M. Zhang, *Ion size and valence effects on ionic flows via Poisson-Nernst-Planck systems*, Commun. Math. Sci., 2017, 15, 881–901.

[9] P. W. Bates, Z. Wen and M. Zhang, *Small permanent charge effects on individual fluxes via Poisson-Nernst-Planck models with multiple cations*, J. Nonlinear Sci., 2021, 31, 1–62.

[10] D. Boda, D. Busath, B. Eisenberg, D. Henderson and W. Nonner, *Monte Carlo simulations of ion selectivity in a biological Na+ channel: Charge-space competition*, Phys. Chem. Chem. Phys., 2002, 4, 5154–5160.

[11] J. Cartailler, Z. Schuss and D. Holcman, *Analysis of the Poisson-Nernst-Planck equation in a ball for modeling the voltage-current relation in neurobiological microdomains*, Phys. D: Nonlinear Phenomena, 2017, 339, 39–48.

[12] D. Chen and R. S. Eisenberg, *Charges, currents and potentials in ionic channels of one conformation*, Biophys. J., 1993, 64, 1405–1421.

[13] J. Chen, Y. Wan, L. Zhang and M. Zhang, *Mathematical analysis of Poisson-Nernst-Planck models with permanent charges and boundary layers: Studies on individual fluxes,* Nonlinearity, 2021, 34, 3879–3906.

[14] J. Ding, Z. Wang and S. Zhou, *Positivity preserving finite difference methods for Poisson-Nernst-Planck equations with steric interaction: application to slit-shaped nanopore conductance*, J. Comput. Phys., 2019, 397, Article ID: 108864.

[15] B. Eisenberg and W. Liu, *Poisson-Nernst-Planck systems for ion channels with permanent charges*, SIAM J. Math. Anal., 2007, 38, 1932–1966.

[16] B. Eisenberg, W. Liu and H. Xu, *Reversal charge and reversal potential: case studies via classical Poisson-Nernst-Planck models*, Nonlinearity, 2015, 28, 103–128.

[17] N. Gavish, *Poisson-Nernst-Planck equations with steric effects- non-convexity and multiple stationary solutions*, Phys. D: nonlinear Phenomena, 2018, 368, 50–65.

[18] N. Gavish, *Poisson-Nernst-Planck equations with high-order steric effects*, Phys. D: nonlinear Phenomena, 2020, 411, Article ID: 132536.

[19] D. Gillespie, *A singular perturbation analysis of the Poisson-Nernst-Planck system: Applications to Ionic Channels*, Ph.D Dissertation, Rush University at Chicago, 1999.

[20] D. Gillespie and R. S. Eisenberg, *Modified Donnan potentials for ion transport through biological ion channels*, Phys. Rev. E, 2001, 63, Article ID: 061902.

[21] D. Gillespie, W. Nonner and R. S. Eisenberg, *Coupling Poisson–Nernst–Planck and density functional theory to calculate ion flux,* J. Phys. Condens. Matter, 2002, 14, 12129–12145.

[22] D. Gillespie, W. Nonner and R. S. Eisenberg, *Density functional theory of charged, hard-sphere fluids*, Phys. Rev. E, 2003, 68, Article ID: 0313503.

[23] A. L. Hodgkin and R. D. Keynes, *The potassium permeability of a giant nerve fibre*, J. Physiol., 1955, 128, 61–88.

[24] U. Hollerbach, D. Chen and R. S. Eisenberg, *Two- and three-dimensional Poisson-Nernst-Planck simulations of current flow through Gramicidian-A*, J. Comput. Sci., 2002, 16, 373–409.

[25] Y. Hyon, B. Eisenberg and C. Liu, *A mathematical model for the hard sphere repulsion in ionic solutions*, Commun. Math. Sci., 2010, 9, 459–475.

[26] Y. Hyon, J. Fonseca, B. Eisenberg and C. Liu, *Energy variational approach to study charge inversion (layering) near charged walls*, Discrete Contin. Dyn. Syst. Ser. B, 2012, 17, 2725–2743.

[27] Y. Hyon, C. Liu and B. Eisenberg, *PNP equations with steric effects: a model of ion flow through channels*, J. Phys. Chem. B, 2012, 116, 11422–11441.

[28] S. Ji, B. Eisenberg and W. Liu, *Flux ratios and channel structures*, J. Dyn. Diff. Equat., 2019, 31, 1141–1183.

[29] S. Ji and W. Liu, *Poisson-Nernst-Planck Systems for Ion Flow with Density Functional Theory for Hard-Sphere Potential: I-V relations and Critical Potentials. Part I: Analysis*, J. Dyn. Diff. Equat., 2012, 24, 955–983.

[30] S. Ji, W. Liu and M. Zhang, *Effects of (small) permanent charges and channel geometry on ionic flows via classical Poisson-Nernst-Planck models*, SIAM J. Appl. Math., 2015, 75, 114–135.

[31] Y. Jia, W. Liu and M. Zhang, *Qualitative properties of ionic flows via Poisson-Nernst-Planck systems with Bikerman's local hard-sphere potential: Ion size effects*, Discrete Contin. Dyn. Syst. Ser. B, 2016, 21, 1775–1802.

[32] J. Kierzenka and L. Shampine, A BVP Solver Based on Residual Control and the Matlab PSE. ACM Trans. Math. Software, 2001, 27, 299–316.

[33] M. S. Kilic, M. Z. Bazant and A. Ajdari, *Steric effects in the dynamics of electrolytes at large applied voltages. II. Modified Poisson-Nernst-Planck equations*, Phys. Rev. E, 2007, 75, Article ID: 021503.

[34] M. G. Kurnikova, R. D. Coalson, P. Graf and A. Nitzan, *A Lattice Relaxation Algorithm for 3D Poisson-Nernst-Planck Theory with Application to Ion Transport Through the Gramicidin A Channel*, Biophys. J., 1999, 76, 642–656.

[35] G. Lin, W. Liu, Y. Yi and M. Zhang, *Poisson-Nernst-Planck systems for ion flow with density functional theory for local hard-sphere potential*, SIAM J. Appl. Dyn. Syst., 2013, 12, 1613–1648.

[36] W. Liu, *Geometric singular perturbation approach to steady-state Poisson-Nernst-Planck systems*, SIAM J. Appl. Math., 2005, 65, 754–766.

[37] W. Liu, *One-dimensional steady-state Poisson-Nernst-Planck systems for ion channels with multiple ion species*, J. Differ. Equations, 2009, 246, 428–451.

[38] J. Liu and B. Eisenberg, *Molecular Mean-Field Theory of Ionic Solutions: a Poisson-Nernst-Planck-Bikerman Model*, Entropy, 2020, 22, 550.

[39] W. Liu, X. Tu and M. Zhang, *Poisson-Nernst-Planck systems for ion flow with density functional theory for hard-sphere potential: I-V relations and critical potentials. Part II: Numerics*, J. Dyn. Diff. Equat., 2012, 24, 985–1004.

[40] W. Liu and B. Wang, *Poisson-Nernst-Planck systems for narrow tubular-like membrane channels*, J. Dyn. Diff. Equat., 2010, 22, 413–437.

[41] W. Liu and H. Xu, *A complete analysis of a classical Poisson-Nernst-Planck model for ionic flow*, J. Differ. Equations, 2015, 258, 1192–1228.

[42] H. Lu, J. Li, J. Shackelford, J. Vorenberg and M. Zhang, *Ion size effects on individual fluxes via Poisson-Nernst-Planck systems with Bikerman's local hard-sphere potential: Analysis without electroneutrality boundary conditions*, Discrete Contin. Dyn. Syst. Ser. B, 2018, 23, 1623–1643.

[43] W. Nooner and R. S. Eisenberg, *Ion permeation and glutamate residues linked by Poisson-Nernst-Planck theory in L-type Calcium channels*, Biophys. J., 1998, 75, 1287–1305.

[44] J. K. Park and J. W. Jerome, *Qualitative properties of steady-state Poisson-Nernst-Planck systems: Mathematical study*, SIAM J. Appl. Math., 1997, 57, 609–630.

[45] S. Sahu and M. Zwolak, *Golden aspect ration for ion transport simulation in nanopores*, Phys. Rev. E, 2018, 98, Article ID: 012404.

[46] Z. Schuss, B. Nadler and R. S. Eisenberg, *Derivation of Poisson and Nernst-Planck equations in a bath and channel from a molecular model*, Phys. Rev. E, 2001, 64, 1–14.

[47] A. Singer and J. Norbury, *A Poisson-Nernst-Planck model for biological ion channels–an asymptotic analysis in a three-dimensional narrow funnel*, SIAM J. Appl. Math., 2009, 70, 949–968.

[48] A. Singer, D. Gillespie, J. Norbury and R. S. Eisenberg, *Singular perturbation analysis of the steady-state Poisson-Nernst-Planck system: applications to ion channels*, European J. Appl. Math., 2008, 19, 541–560.

[49] M. Valiskó, B. Matejczyk, Z. Ható, T. Kristóf, E. Mádai, D. Fertig, D. Gillespie and D. Boda, *Multiscale analysis of the effect of surface charge pattern on a nanopore's rectification and selectivity properties: From all-atom model to Poisson-Nernst-Planck*, J. Chem. Phys., 2019, 150, Article ID: 144703.

[50] X. Wang, D. He, J. Wylie and H. Huang, *Singular perturbation solutions of steady-state Poisson-Nernst-Planck systems*, Phys. Rev. E, 2014, 89, 1–14.

[51] Z. Wen, P. W. Bates and M. Zhang, *Effects on I-V relations from small permanent charge and channel geometry via classical Poisson-Nernst-Planck equations with multiple cations*, Nonlinearity, 2021, 34, 4464–4502.

[52] Z. Wen, L. Zhang and M. Zhang, *Dynamics of classical Poisson-Nernst-Planck systems with multiple cations and boundary layers*, J. Dyn. Diff. Equat., 2021, 33, 211–234.

[53] M. Zhang, *Asymptotic expansions and numerical simulations of I-V relations via a steady-state Poisson-Nernst-Planck system*, Rocky MT. J. Math., 2015, 45, 1681–1708.

[54] M. Zhang, *Boundary layer effects on ionic flows via classical Poisson-Nernst-Planck systems*, Comput. Math. Biophys., 2018, 6, 14–27.

[55] M. Zhang, *Competition between cations via Poisson-Nernst-Planck systems with nonzero but small permanent charges*, Membranes, 2021, 11, 236.